Downregulation of long non-coding RNA MR4435-2HG suppresses breast cancer progression via the Wnt/β-catenin signaling pathway

DEQIN CHEN[1], PENGTING TANG[2], YIKE WANG[1], FANG WAN[1], JINGPEI LONG[1], JUN ZHOU[1], MING ZHUANG[3] and XIN CHEN[1]

[1]Department of Surgery, The Women's Hospital, School of Medicine, Zhejiang University, Hangzhou, Zhejiang 310006; [2]Department of Surgery, Ninghai Maternity and Child Care Hospital, Ningbo, Zhejiang 315600; [3]Department of Breast Surgery, Xinhua Hospital Affiliated to Shanghai Jiao Tong University School of Medicine, Shanghai 200092, P.R. China

Received May 30, 2020; Accepted February 9, 2021

DOI: 10.3892/ol.2021.12634

Abstract. Extensive research has contributed to the current understanding of the critical roles played by long non-coding RNAs in various types of cancer. The present study aimed to investigate the function and mechanism of the long non-coding RNA, MIR4435-2HG (also termed LINC00978), in breast cancer growth and metastasis. Using Gene Expression Profiling Interactive Analysis, an online web tool, it was revealed that MIR4435-2HG was upregulated in breast cancer tissue, and its high expression was associated with poor prognosis based on The Cancer Genome Atlas database. MIR4435-2HG knockdown increased cell apoptosis but decreased cell proliferation, migration and invasion. MIR4435-2HG knockdown increased pro-apoptotic protein expression but decreased anti-apoptotic protein expression. In addition, MIR4435-2HG knockdown leads to dysregulation of epithelial-to-mesenchymal transition-associated genes. Furthermore, knockdown of MIR4435-2HG results in inactivation of the Wnt/β-catenin signaling pathway. The results of the present study demonstrate the tumor-promoting role of MIR4435-2HG in breast cancer progression.

Introduction

Breast cancer is the most commonly diagnosed malignancy in women, with 21.6 new cases and 5.7 mortalities per 100,000 women reported in China in 2008 (1). In recent years, the incidence and mortality rates of breast cancer has increased, posing a threat to the physical and mental health of women worldwide. Globally, ~1.7 million new cases of breast cancer are diagnosed, with 521,900 deaths every year (2). Over the past two decades, great progress has been achieved in the early diagnosis and treatment of breast cancer through combining surgery, adjuvant therapy and hormone therapy; however, the overall prognosis of breast cancer remains poor due to late diagnoses, frequent recurrence and high chemoresistance (3-6). Therefore, understanding the underlying mechanisms of breast cancer progression is urgently required. Doing so may aid in identifying new biomarkers for early diagnosis and prognosis prediction.

Long non-coding RNAs (lncRNAs) are >200 nucleotides in length, but without the protein-coding ability (7), are aberrantly expressed and play critical regulatory roles in multiple types of cancer by regulating tumor growth, metastasis and metabolism (8,9). In breast cancer, a number of individual lncRNAs are dysregulated and contribute to tumor progression. For example, LINC01121 mediates the expression of HMGA2 to promote breast cancer cell proliferation, migration and invasion by sponging microRNA (miR/miRNA)-150-5p (10). In addition, the nuclear LINC00993, which is downregulated in breast cancer tissue, inhibits triple-negative breast cancer growth both *in vitro* and *in vivo* by orchestrating the expression of cell cycle regulators (11). The lncRNA GAEA interacts with MEX3C to enhance the K27-linked polyubiquitination of PTEN, consequently activating the epithelial-to-mesenchymal transition (EMT) process (12). MALAT1, which is upregulated in breast cancer tissues, promotes tumor development and progression both *in vitro* and *in vivo* (13). However, functions of the vast majority of lncRNAs have not yet been characterized.

MIR4435-2HG (also named LINC00978 or AK001796), a lncRNA that is located in the 2q13 region, has been shown to function as a tumor promoter in various types of cancer (14-17). MIR4435-2HG interacts with EZH2 to inhibit p21 and E-cadherin expression, promoting the progression of hepatocellular carcinoma (HCC) (14). Through activating β-catenin

Correspondence to: Dr Ming Zhuang, Department of Breast Surgery, Xinhua Hospital Affiliated to Shanghai Jiao Tong University School of Medicine, Building 8, 1665 Kongjiang Road, Shanghai 200092, P.R. China
E-mail: zhuangming@xinhuamed.com.cn

Dr Xin Chen, Department of Surgery, The Women's Hospital, School of Medicine, Zhejiang University, 1 Xueshi Road, Hangzhou, Zhejiang 310006, P.R. China
E-mail: 5313014@zju.edu.cn

Key words: breast cancer, MIR4435-2HG, proliferation, metastasis, Wnt/β-catenin

signaling and inhibiting miR-6754-5p, MIR4435-2HG promotes lung cancer progression (15,16). Additionally, a previous study revealed that MIR4435-2HG was upregulated in gastric cancer and promotes tumor growth and metastasis via activating the Wnt/β-catenin signaling pathway (17). Several recent reports (18,19) have revealed that MIR4435-2HG was involved in the regulation of cell apoptosis. Knockdown of MIR4435-2HG in cisplatin-resistant cell line HCT116R significantly promoted cell apoptosis and restored the sensitivity to cisplatin (18). MIR4435-2HG knockdown induced ovarian cancer cell apoptosis via the miR-128-3p/CDK14 axis (19). Therefore, targeting MIR4435-2HG using antisense oligonucleotides to induce apoptosis may be a potential advancement in cancer drug development. Notably, Deng *et al* (20) reported that MIR4435-2HG is highly expressed in breast cancer cell lines and tissues, and could be utilized to predict prognosis in patients with breast cancer. However, the biological functions and underlying mechanisms of breast cancer remain to be elucidated.

The aim of the present study was to investigate the function of MIR4435-2HG and its associated signaling pathways in breast cancer. In addition, the effects of MIR4435-2HG knockdown on cell proliferation, apoptosis and migration were elucidated. The mechanisms by which MIR4435-2HG promotes tumor progression have been explored in the present study. The findings of the present study suggested that MIR4435-2HG may be a promising therapeutic target for breast cancer.

Materials and methods

RNA isolation and reverse transcription-quantitative PCR (RT-qPCR). Using TRIzol® reagent (Invitrogen; Thermo Fisher Scientific, Inc.), total RNA was extracted from MCF-7 and MDA-MB-231 cells according to the manufacturer's protocol. The first-strand cDNA was generated from 1 μg total RNA using the PrimeScript RT reagent kit (Takara Bio, Inc.) according to the manufacturer's protocol. For the RT-qPCR, SYBR Green Premix Ex Taq (Takara Bio, Inc.) was used according to the manufacturer's protocol. The relative expression levels of target genes were calculated using the $2^{-\Delta\Delta Cq}$ method (21) with GAPDH as an endogenous reference gene. The primer sequences used in the present study were as follows: MIR4435-2HG: Forward, 5'-AGGCCCCAG GGAATCTTTCA-3' and reverse, 5'-GCCTCTCCCTGAATA ACTGGG-3'; GAPDH: Forward, 5'-GGAGCGAGATCCCTC CAAAAT-3' and reverse, 5'-GGCTGTTGTCATACTTCT CATGG-3'. The experiments were performed three times, and the RT-qPCR assays were performed in triplicate.

Lentivirus-mediated RNA interference. The sequence for the short hairpin (sh) RNA targeting MIR4435-2HG was: 5'-CACCGCCCAGATTTAAGGGCTATTTCA AGAGAATAGCCCTTAAATCTGGGCCTTTTTTG-3' as previously reported (14), and the negative control sequence (shNC) was 5'-CACCGTTCTCCGAACGTGTCACGTCAA GAGATTACGTGACACGTTCGGAGAATTTTTTG-3'. The shMIR4435-2HG (1 μg) and shNC (1 μg) were synthesized and inserted into the lentivirus core vector that contained an enhanced green fluorescent protein (EGFP) reporter gene, hU6-MCS-CMV-EGFP. Recombinant lentiviruses expressing shMIR4435-2HG or the empty lentiviral vector shNC were produced by Shanghai Genechem Co., Ltd. Then, $6x10^5$ cells were infected with concentrated lentivirus (MOI=40) in the presence of 8 μg/ml of polybrene (Sigma Aldrich; Merck KGaA). After 72 h incubation, cells were selected using puromycin (1 μg/ml; Sigma Aldrich; Merck KGaA) for 5 days. To evaluate the expression level of MIR4435-2HG, RT-qPCR was used.

Cell apoptosis assay. Apoptotic cells were assessed using an annexin V-FITC/propidium iodide apoptosis detection kit (Abcam) via flow cytometry in MDA-MB-231 and MCF-7 cells (Cell Bank of Type Culture Collection of the Chinese Academy of Sciences). Since shRNA lentivirus vector expressing GFP will influence the FACS signal of Annexin-FITC, siRNA was used to knock down MIR4435-2HG in the flow cytometric analysis of apoptotic assays. Briefly, breast cancer cells ($5x10^4$ cells/ml) transfected with 50 nM siMIR4435-2HG (5'-CCCAGAUUU AAGGGCUAUUTT-3') or siNC (5'-UUCUCCGAACGUGUC ACGUTT-3') were seeded in 6-well culture plates. After 48 h, cells were digested by 0.25% EDTA-free trypsin, washed 2 times with cold PBS, resuspended in 100 μl binding buffer, and stained with Annexin V-FITC as well as propidium iodide (100 μg/ml). After 15 min incubation at 37˚C in the dark, apoptotic cells were analyzed using a FACS Calibur flow cytometer (Becton, Dickinson and Company), and analyzed using Cell Quest software v.3.3 (Becton, Dickinson and Company). The experiment was performed in triplicate.

Cell culture and growth conditions. Human transformed mammary epithelial cell line (MCF-10A) and human breast cancer cell lines (MDA-MB-231 and MCF-7) were obtained from the Cell Bank of Type Culture Collection of the Chinese Academy of Sciences. MDA-MB-231 and MCF-7 cells were cultured in high-glucose Dulbecco's modified Eagle's medium (DMEM) supplemented with 10% fetal bovine serum (FBS; Gibco; Thermo Fisher Scientific, Inc.) in the presence of 1% penicillin/streptomycin. (Sigma-Aldrich; Merck KGaA). MCF-10A cells were cultured in DMEM-F12 (Gibco; Thermo Fisher Scientific, Inc.) supplemented with 10% FBS in the presence of 100 U/ml penicillin, 100 μg/ml of streptomycin, 20 ng/ml of epidermal growth factor and 2 mM of L-glutamine. All cells were cultured at 37˚C with 5% CO_2 in a standard cell culture incubator (Thermo Fisher Scientific, Inc.).

Cell Counting Kit-8 (CCK-8) assays. Cell proliferation was detected using CCK-8 assays (Dojindo Molecular Technologies Inc.). Briefly, cells were seeded in 96-well plates at a density of 1,000 cells/well. At each time point (0, 1, 2, 3, 4 and 5 days), culture medium was replaced with 100 μl DMEM supplemented with 10 μl CCK-8 reagent (Dojindo, Japan). Cells were then incubated at 37˚C for 2 h, and then the absorbance was measured at 450 nm. Cell proliferation rate was calculated relative to day 0 (6 h after seeding), which were the controls.

Colony formation assays. A total of 500 cells were seeded per well onto 6-well plates. The medium was replenished with fresh medium every 3 days. After 14 days culture, the medium was removed and the cells were fixed with 4% paraformaldehyde

for 20 min at 4˚C after washing twice with PBS, stained with 0.1% crystal violet (Beyotime Institute of Biotechnology) for 20 min at room temperature. After another wash with water, cells were air-dried, and colonies containing >50 cells were counted manually. Images of the representative single colony was captured using a light microscope (magnification, x100).

Western blot analysis. Total protein was extracted from MDA-MB-231 and MCF-7 cells infected with shMIR4435-2HG- or shNC-viruses using RIPA lysis buffer (Beyotime Institute of Biotechnology). To extract cytoplasmic and nuclear proteins, cytoplasmic and nuclear extracts were prepared using a Nuclear and Cytoplasmic Extraction kit (Beyotime Institute of Biotechnology) according to the manufacturer's instructions. The protein concentration of the soluble materials was measured using a BCA protein assay kit (Beyotime Institute of Biotechnology), with bovine serum albumin (Beyotime Institute of Biotechnology) serving as a standard. Then, the proteins (40 μg per lane) were separated via 10% SDS-PAGE and then transferred onto a polyvinylidene difluoride (PVDF) membrane (EMD Millipore). The membranes were blocked in 5% fat-free milk at room temperature for 1 h followed by incubating with specific primary antibodies at 4˚C overnight, including the anti-β-actin (1:5,000; cat. no. ab8227; Abcam), anti-PCNA (1:1,000; cat. no. ab92552; Abcam), anti-GAPDH (1:1,000; cat. no. ab9485; Abcam), anti-ZEB1 (1:1,000; cat. no. 3396; Cell Signaling Technology, Inc.), anti-E-cadherin (1:1,000; cat. no. 3195; Cell Signaling Technology, Inc.), anti-Lamin B1 (1:1,000; cat. no. ab133741; Abcam), anti-N-cadherin (1:1,000; cat. no. 14215; Cell Signaling Technology, Inc.), anti-Bax antibody (1:1,000; cat. no. 5023; Cell Signaling Technology), anti-Bcl-2 (1:1,000; cat. no. 4223; Cell Signaling Technology, Inc.), anti-Cleaved-caspase-3 (1:1,000; cat. no. 9661; Cell Signaling Technology, Inc.), anti-β-catenin (1:1,000; cat. no. ab68183; Abcam), anti-cleaved-PARP (1:1,000; cat. no. 5625; Cell Signaling Technology, Inc.) and anti-vimentin (1:1,000; cat. no. 5741; Cell Signaling Technology, Inc.). Horseradish peroxidase-conjugated anti-rabbit (1:1,000; cat. no. BA1054, Wuhan Boster Biological Technology, Inc.) or mouse secondary antibodies (1:1,000; cat. no. BA1050, Wuhan Boster Biological Technology, Inc.) were added and incubated at room temperature for 1 h. Detection was performed using the ECL reagent (Pierce; Thermo Fisher Scientific, Inc.). Protein levels were quantified through densitometry using Photoshop CS4 version v.11.0.1 (Adobe, Systems, Inc.).

Transwell cell migration and basement membrane matrix invasion assay. Migration and invasion assays were performed to evaluate the effect of MIR4435-2HG on breast cancer cell metastasis. Briefly, the Transwell inserts (Costar; Corning, Inc.) with 8 μm pore polycarbonate membranes (Corning, Inc.) coated with Matrigel at 37˚C for 4 h or without Matrigel (BD Biosciences) were used in the invasion and migration assays, respectively. MDA-MB-231 and MCF-7 cells infected with shNC or shMIR4435-2HG viruses were resuspended in a serum-free medium and further $6x10^4$ cells for MCF-7 or $2x10^4$ cells for MDA-MB-231 were seeded into the upper chamber of the Transwell insert. The lower chamber was filled with 500 μl DMEM (Gibco; Thermo Fisher Scientific, Inc.) containing 10% FBS (Gibco; Thermo Fisher Scientific, Inc.). After 24 h incubation at 37˚C with 5% CO_2, cells in the upper chamber were gently removed using a cotton swab, whereas cells in the lower chamber were washed with PBS, fixed with 4% paraformaldehyde at 4˚C for 20 min, and stained with 0.1% crystal violet at room temperature for 20 min. Eventually, cells that had migrated/invaded into the filter were counted and analyzed. Images of the representative migrative or invasive pictures were captured using a light microscope (magnification, x100). Each assay was performed in triplicate.

Bioinformatics/database analysis. Data from the Gene Expression Profiling Interactive Analysis (GEPIA) database (http://gepia.cancer-pku.cn/index.html) were used to analyze the differential expression of MIR4435-2HG and its prognostic values in breast cancer. A gene symbol (MIR4435-2HG) was entered into the 'Enter gene name' field. Then the 'GoPIA!' button was clicked to obtain the expression profile of the input gene across all tumor and normal tissues. For the profile of MIR4435-2HG expression, input 'MIR4435-2HG' under 'Gene', the 'ANOVA' option was selected under 'Differential Methods', choose 'No' under 'Log Scale', choose 'Match TCGA normal data' under 'Matched Normal data', the 'BRCA' option was selected under 'Cancer name'; click 'Plot' button and the results were then displayed. For the boxplot of MIR4435-2HG expression, the 'Boxplot' tab under the 'Expression DIY' section was clicked, the 'BRCA' option was selected under 'Cancer name', choose 'Yes' under 'Log Scale', set 'Jitter size' as '0.4', and choose 'Match TCGA normal data' under 'Matched Normal data'; the results were then displayed in box plots. For the survival analysis, click the 'Survival Plots' tab under the 'Survival' section, the 'Overall Survival' or 'Disease Free Survival (DFS)' was selected under 'Methods', choose 'Quartile' as the cut-off value to separate patients into high (>75% quartile) and low (<25% quartile) expression groups, choose 'No' under 'Hazards Ratio (HR)', choose 'No' under '95% Confidence Interval', choose 'months' under 'Axis Units', and the 'BRCA' option was selected under 'Cancer name'; click 'Plot' button and the results were then displayed.

Statistical analysis. Data are expressed as the mean ± standard deviation from three independent experiments unless otherwise stated. To determine statistical significance, an unpaired Student's t-test or one-way ANOVA (with Tukey's post hoc test) was used and analyzed using GraphPad Prism software (version 5.0; GraphPad Software) and SPSS software (version 22.0; IBM Corp.). Kaplan-Meier analysis was used to evaluate disease-free survival rate and overall survival rate. $P<0.05$ was considered to indicate a statistically significant difference.

Results

MIR4435-2HG is upregulated in breast cancer tissue and its high expression level is associated with poor prognosis. A previous report showed that MIR4435-2HG is highly expressed in breast cancer tissues (n=36) compared with adjacent normal tissues (20). To confirm this observation, the present study retrieved and analyzed the expression

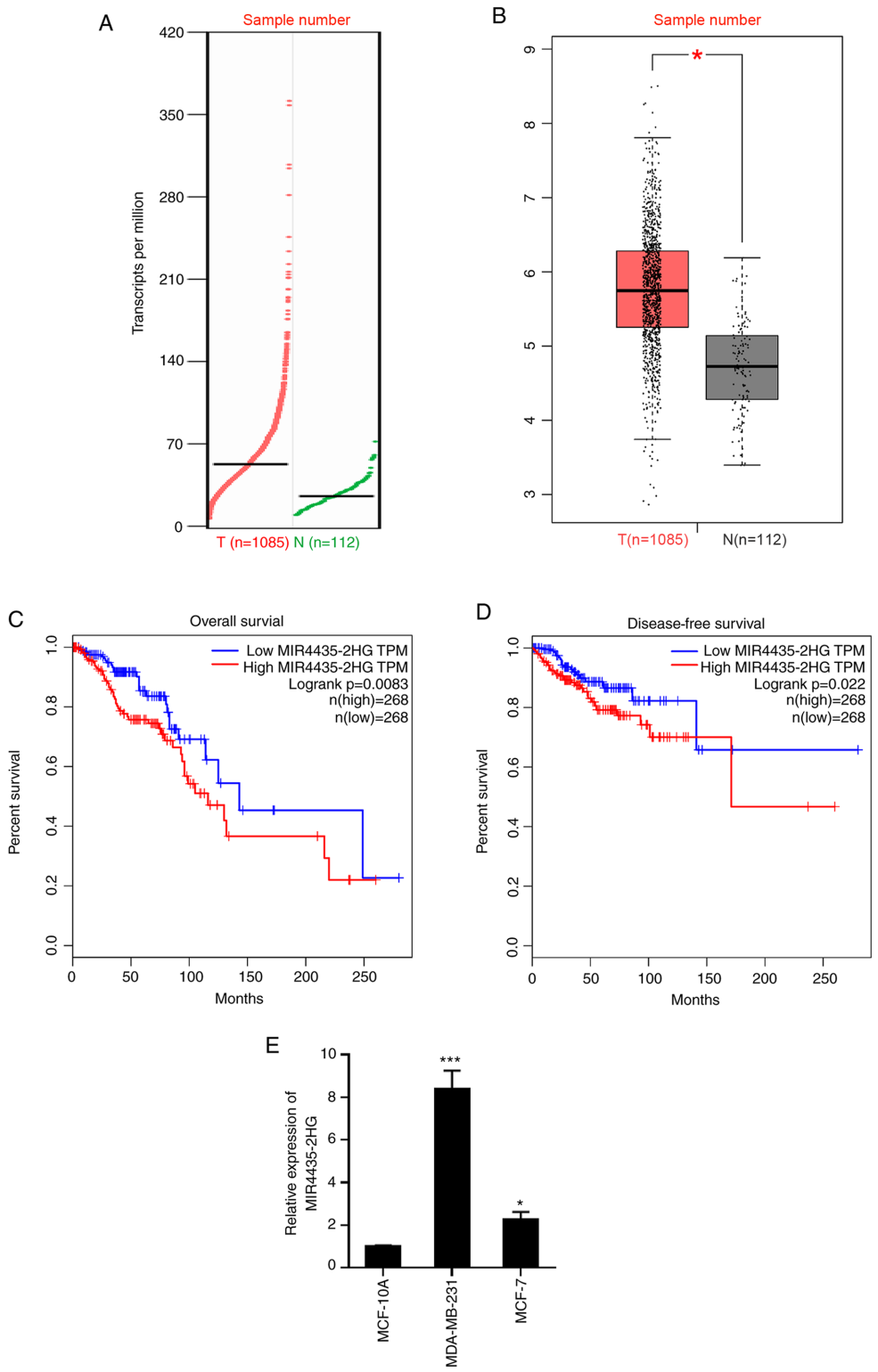

Figure 1. MIR4435-2HG expression is increased in breast cancer tissue and breast cancer cell lines. (A) Dot plot of the MIR4435-2HG expression profile across breast cancer tissues (red, n=1,085) and normal tissues (green, n=112) based on GEPIA database. (B) Box plot of MIR4435-2HG expression in breast cancer tissues (n=1,085) and normal tissues (n=112) based on the GEPIA database. Kaplan-Meier (C) overall survival and (D) disease-free survival in patients with breast cancer stratified by MIR4435-2HG expression. (E) Reverse transcription-quantitative PCR analysis of MIR4435-2HG expression in the indicated cells with GAPDH serving as the internal control. *P<0.05, ***P<0.001 vs. MCF-10A. GEPIA, Gene Expression Profiling Interactive Analysis.

level of MIR4435-2HG in a large cohort of samples from patients with breast cancer based on The Cancer Genome Atlas database using the online web portal GEPIA (http://gepia.cancer-pku.cn/index.html) (22). As presented in Fig. 1A and B, MIR4435-2HG expression was significantly upregulated in breast cancer tissues compared with normal tissues (P<0.05). Kaplan-Meier analysis demonstrated that patients with higher MIR4435-2HG expression levels exhibited decreased overall survival times (P=0.0083) and shorter disease-free survival times (P=0.022)

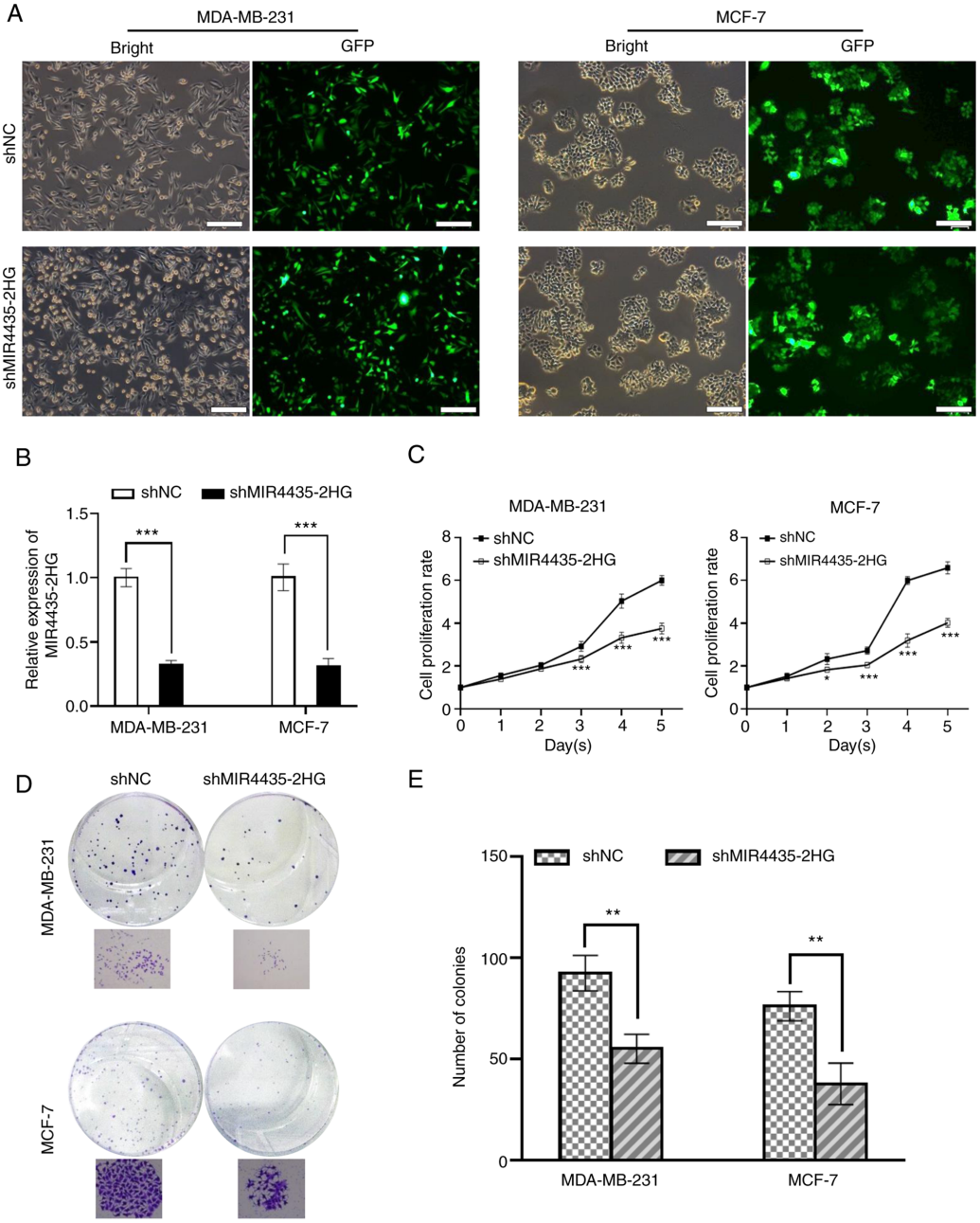

Figure 2. Knockdown of MIR4435-2HG suppresses the proliferation of breast cancer cells. (A) MDA-MB-231 and MCF-7 cells were infected with shMIR4435-2HG or shNC lentivirus (scale bar, 200 μm). (B) Reverse transcription-quantitative analysis of MIR4435-2HG expression in indicated cells with GAPDH serving as an internal control. (C) The cell viability was detected by Cell Counting Kit-8 assay in MCF-7 and MDA-MB-231 cells following MIR4435-2HG knockdown. (D) Knockdown of MIR4435-2HG decreased the colony formation activity of MDA-MB-231 and MCF-7 cells, as determined by a colony formation assay. Images of the stained cell colonies were captured. (E) The number of colonies were calculated and statistically analyzed. *P<0.05, **P<0.01 and ***P<0.001 vs. shNC. sh, short hairpin; NC, negative control; GFP, green fluorescent protein.

(Fig. 1C and D). In addition, the RT-qPCR analysis revealed that MIR4435-2HG expression was higher in breast cancer cell lines when compared with that in the normal breast cell line MCF-10A (Fig. 1E). Taken together, these data suggest that MIR4435-2HG may function as an oncogene in breast cancer and its high expression is associated with poor prognosis of patients with breast cancer.

Inhibition of MIR4435-2HG suppresses the proliferation of breast cancer cells. To investigate the potential function of MIR4435-2HG in breast cancer, the present study performed MIR4435-2HG-knockdown in MDA-MB-231 and MCF-7 cells by lentiviral infection (shMIR4435-2HG) with an empty lentiviral vector as the shNC. Fluorescence detection showed that the transfection efficiency was >90% according to the ratio of GFP positive cells in both cell lines (Fig. 2A). Furthermore, RT-qPCR analysis showed that MIR4435-HG transcript levels were decreased by ~70% in MDA-MB-231 and MCF-7 cells expressing shMIR4435-2HG compared with the shNC group (P<0.01; Fig. 2B). In order to investigate the effects of MIR4435-2HG on cell proliferation, CCK-8 and colony formation assays were performed in MDA-MB-231 and MCF-7 cells. The results revealed that MIR4435-2HG-depleted MDA-MB-231 or MCF7 cells

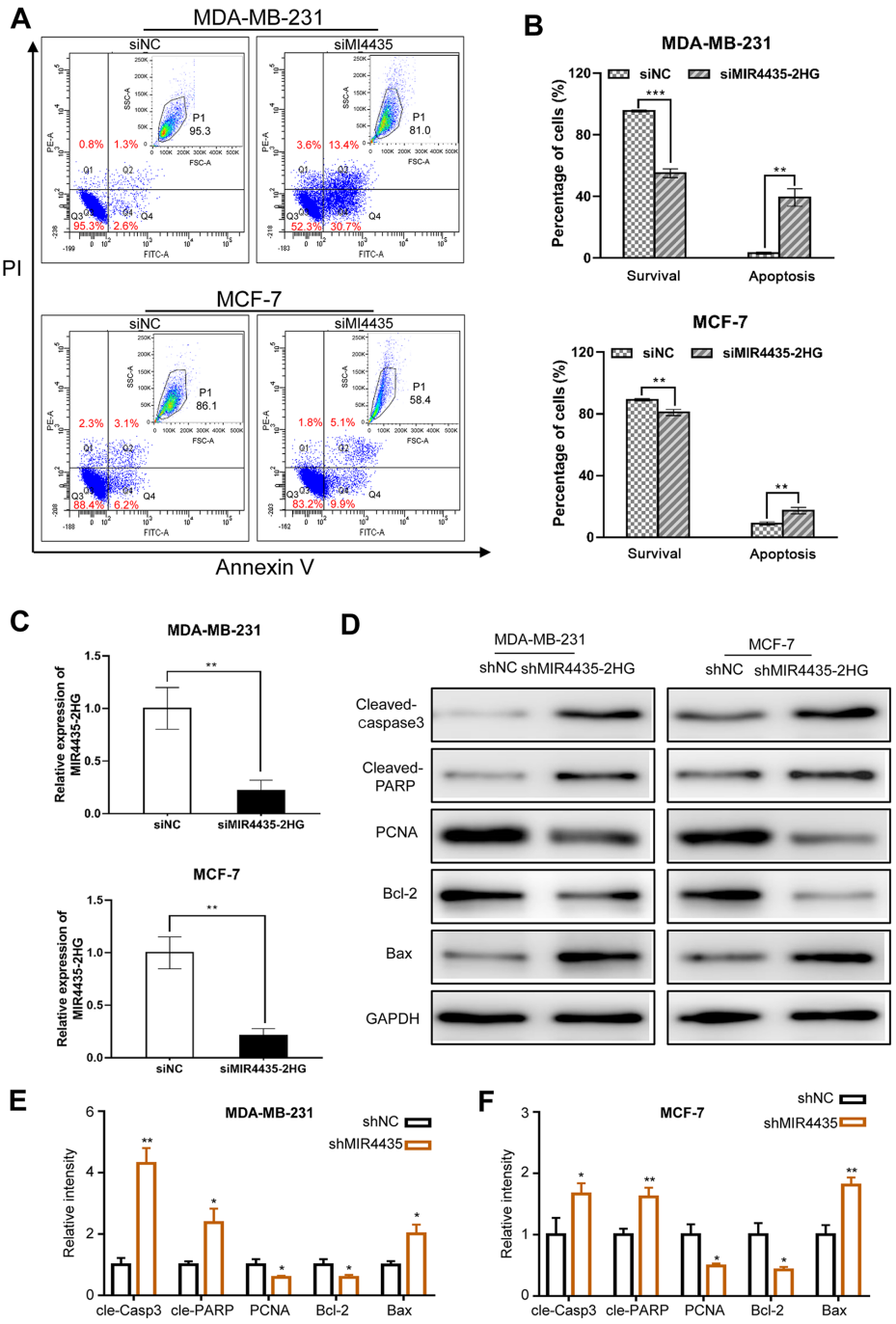

Figure 3. Knockdown of MIR4435-2HG enhances cell apoptosis in breast cancer cells. (A) After 48 h transfection, cells were labelled with Annexin V-FITC and PI and then cell apoptosis was analyzed by flow cytometry. The original flow cytometry plots are shown in the upper-right panel of each dot plots. (B) The percentage of apoptotic cells was calculated. The data are presented as the mean ± standard deviation. (C) Reverse transcription-quantitative PCR analysis of MIR4435-2HG expression following transfection of si-NC or si-MIR4435-2HG with GAPDH serving as the internal control. (D) Protein expression levels of cleaved-PARP, PCNA, Bcl-2, Bax and cleaved-caspase 3 was measured by western blotting in MDA-MB-231 cells (left panel) and MCF-7 cells (right panel). (E and F) Relative density of indicated proteins in (D) *P<0.05, **P<0.01, ***P<0.001 vs. shNC. PI, propidium iodide; si, small interfering; sh, short hairpin; NC, negative control.

proliferated significantly slower than control cells (P<0.01 and P<0.05). Furthermore, shMIR4435-2HG-MDA-MB-231 or MCF7 cells had significantly fewer and smaller sized colonies than control cells (P<0.01; Fig. 2D and E). Based on these results, it was concluded that MIR4435-2HG exerts a crucial role in breast cancer cell proliferation, and that targeting MIR4435-2HG may effectively inhibit breast cancer progression.

Effect of MIR4435-2HG on breast cancer cell apoptosis. The effects of MIR4435-2HG on cell apoptosis were assessed via flow cytometry analyses (Fig. 3A). As presented in Fig. 3B and C, MIR4435-2HG knockdown significantly increased the proportions of apoptotic MDA-MB-231 and MCF-7 cells compared with siNC-transfected cells (P<0.05). To gain further insight into the molecular mechanism by which shMIR4435-2HG induces apoptosis of breast cancer cells,

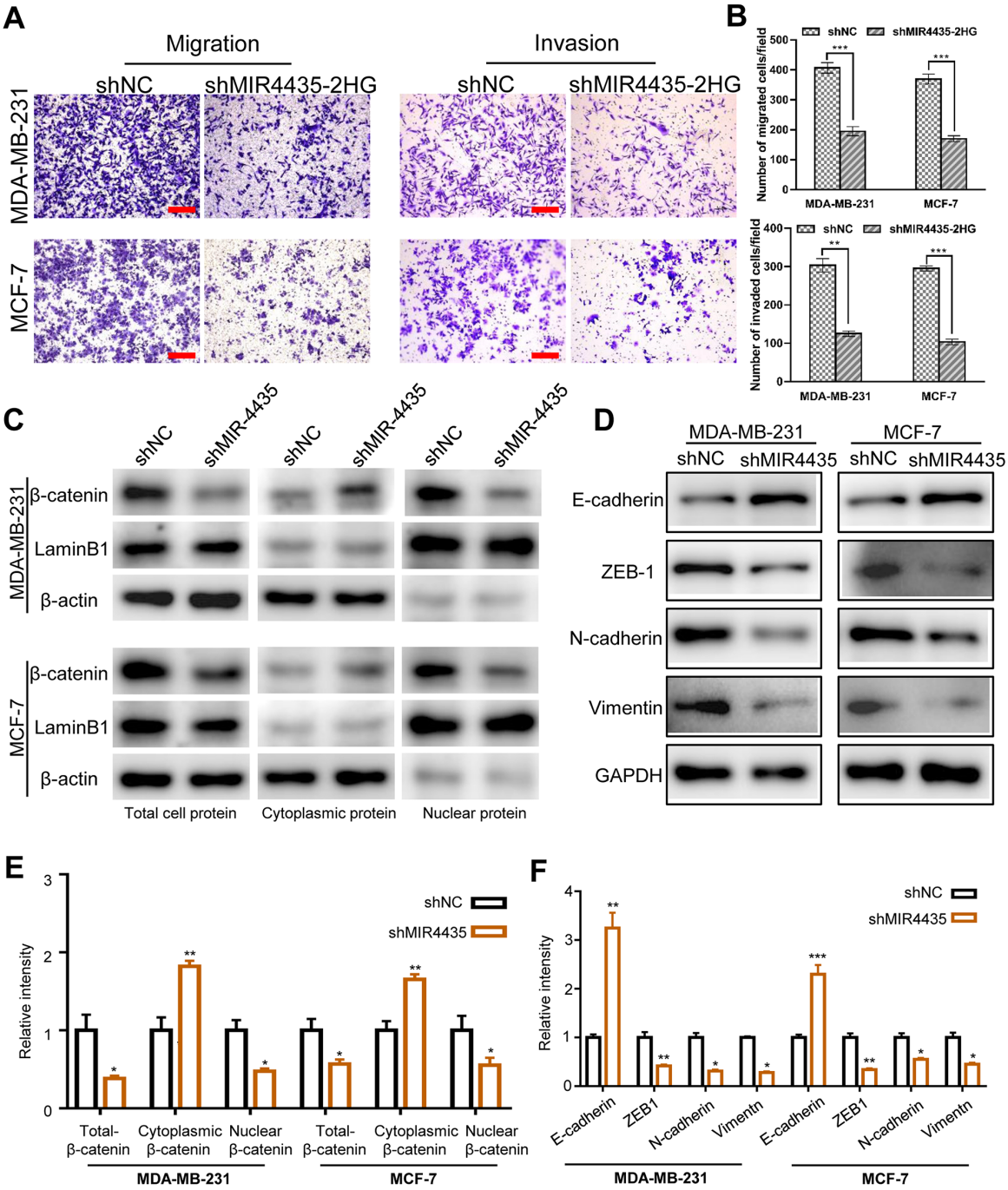

Figure 4. Knockdown of MIR4435-2HG attenuates tumor metastasis and invasion via the Wnt/β-catenin signaling pathway. (A) Transwell migration (upper panel) and invasion assays (bottom panel) were performed to measure the effects of MIR4435-2HG downregulation on the migration and invasion abilities of MDA-MB-231 and MCF-7 cells. Scale bar, 100 μm. (B) Migrated and invaded cells were counted in five random fields. (C) Total, cytoplasmic and nuclear β-catenin expression levels were determined via western blotting after inhibiting MIR4435-2HG. LaminB1 and GAPDH served as nuclear and cytoplasmic markers, respectively. (D) Expression levels of E-cadherin, ZEB1, N-cadherin and vimentin in MDA-MB-231 and MCF-7 cells infected with MIR4435-2HG shRNA or shNC. GAPDH was served as internal control. (E) Relative density of indicated proteins in (C). (F) Relative density of indicated proteins in (D). *P<0.05, **P<0.01, ***P<0.001 vs. shNC. sh, short hairpin; NC, negative control.

the present study measured the expression levels of several apoptosis-associated proteins post-silencing MIR4435-2HG. The western blot results revealed that the expression levels of Bcl-2, an anti-apoptotic marker, and the proliferating marker PCNA, were decreased significantly in MDA-MB-231 and MCF-7 cells after inhibiting MIR4435-2HG. While the expression of cleaved-PARP, cleaved-caspase-3 and Bax, which were makers of activation of apoptosis pathways, were upregulated upon MIR4435-2HG knockdown (Fig. 3D and F). These findings suggested that knockdown of MIR4435-2HG induces apoptosis through downregulation of anti-apoptotic proteins and upregulation of proapoptotic proteins in breast cancer cells.

Knockdown of MIR4435-2HG inhibits breast cancer cell metastasis and invasion via the Wnt/β-catenin pathway. The present study performed transwell assays to investigate the

effect of MIR4435-2HG on the migration and invasion of breast cancer cells. As presented in Fig. 4A and B, MDA-MB-231 and MCF-7 cells displayed significantly lowered migration and invasion capabilities compared with the control cells upon MIR4435-2HG silencing. A previous study reported that MIR4435-2HG could inhibit gastric cancer progression through inactivating Wnt/β-catenin pathway (17). Given that dysregulation of Wnt/β-catenin pathway has been shown to be involved in the progression of various types of tumor, including breast cancer (23), the present study examined whether MIR4435-2HG could regulate breast cancer metastasis by altering the Wnt/β-catenin signaling pathway. Following the western blot analyses, it was revealed that MIR4435-2HG knockdown decreased total and nuclear β-catenin expression, and slightly elevated the cytoplasmic β-catenin expression (Fig. 4C and E). The present study also assessed the expression of EMT-associated proteins via western blotting. As presented in Fig. 4D and F, MIR4435-2HG knockdown attenuated the expression of N-cadherin, ZEB1and vimentin, whereas E-cadherin expression was enhanced. Collectively, the aforementioned findings demonstrate that MIR4435-2HG contributed to breast cancer cell metastasis through orchestrating Wnt/β-catenin signaling.

Discussion

It has previously been described that MIR4435-2HG is upregulated and plays crucial roles in HCC (14), lung cancer (15), ovarian cancer (24), prostate cancer (25) and gastric cancer (17). Notably, MIR4435-2HG expression is increased in breast cancer tissues and is associated with poor prognosis (20). However, whether MIR4435-2HG affects the biological function of breast cancer cells remains to be elucidated. To the best of our knowledge, the present study it the first to report on the oncogenic function of MIR4435-2HG in breast cancer cells.

Apoptosis failure, as one of the hallmarks of cancer (also referred to as genetically programmed cell death), has been extensively demonstrated to be executed upon the cleavage of a series of cysteine proteases termed pro-caspases (26). The initiators caspase-8 and -9 are the first to be activated during apoptosis, and they subsequently activate the executioners caspase-3 and -7, which are responsible for the cleavage of several downstream substrates, including the PARP protein, ultimately activating apoptosis (27,28). Activation of caspase-3 could cleave BID to promote the mitochondrial apoptosis pathway (29). In the present study, it was revealed that MIR4435-2HG knockdown causes the upregulation of cleaved-PARP and cleaved caspase-3. Furthermore, MIR4435-2HG knockdown increased the expression of pro-apoptotic protein Bax and decreased the expression of anti-apoptotic protein Bcl-2 in breast cancer cells. The results of the present study suggest that the mitochondrial pathway is associated with MIR4435-2HG knockdown-mediated apoptosis in breast cancer cells.

Increasing evidence indicates that the EMT plays a crucial role in the metastasis of breast cancer. EMT is a complex, reversible and multi-step biological event characterized by the loss of apical polarity and cell-cell contacts and acquired mesenchymal phenotypes of mobility, plasticity and stem cell-like properties (30,31). Notably, EMT may occur under physiological processes, such as embryogenesis and wound healing; however, it is active during carcinogenesis, thereby conferring the invasive and metastatic abilities of tumor cells (32). As EMT occurs, the mesenchymal protein markers N-cadherin and vimentin are increased and concurrently, the epithelial protein marker E-cadherin is decreased (33). In the present study, it was revealed that MIR4435-2HG knockdown significantly decreased the expression of mesenchymal markers, including N-cadherin, vimentin and ZEB1, whereas it augmented expression of epithelial marker E-cadherin. These results indicate that MIR4435-2HG promotes metastasis by driving EMT in breast cancer cells. Based on a previous report, MIR4435-2HG could inhibit gastric cancer progression through inactivating Wnt/β-catenin pathway (17). Consistently, the results of the present study also demonstrated that knockdown of MIR4435-2HG resulted in a decrease of total and nuclear β-catenin expression. The Wnt/β-catenin signaling pathway has been shown to be involved in the anti-apoptotic function of cells (34-36). Arsenic trioxide (ATO) significantly induced HeLa cell apoptosis via decreasing β-catenin expression at both the mRNA and protein levels (34). Triptolide induces breast cancer cell apoptosis by suppressing the Wnt/β-catenin signaling pathway (35). The generation of reactive oxygen species by thalidomide suppressed the Wnt/β-catenin signaling pathway, with subsequent activation of the intrinsic apoptotic pathway (36). However, whether other signaling pathways are involved in MIR4435-2HG-mediated tumor progression need to be further investigated. Several previous reports have demonstrated that MIR4435-2HG promotes cancer progression via activating the TGF-β signaling pathway in prostate and lung cancer (25,37). Thus, it would be of great importance to investigate whether MIR4435-2HG modulates this pathway in breast cancer. In addition, Kong *et al* (38) demonstrates that MIR4435-2HG promotes HCC cell proliferation by upregulating miRNA-487a. Therefore, it is rational to hypothesize that MIR4435-2HG may modulate miRNA expression in breast cancer. Taken together, the present study provides new insight into the oncogenic roles of MIR4435-2HG in breast cancer progression, and thus may be utilized as a critical therapeutic target for breast cancer treatment. However, additional studies are needed to fully understand the molecular mechanisms of MIR4435-2HG-mediated tumor progression.

In conclusion, the present study demonstrated that MIR4435-2HG was upregulated in breast cancer and predicts poor prognosis. Notably, MIR4435-2HG knockdown promotes cell apoptosis but inhibits breast cancer cell proliferation, migration and invasion by impeding the Wnt/β-catenin axis. These results suggested the potential value of MIR4435-2HG as a novel promising diagnostic, therapeutic and prognostic target for the treatment of breast cancer.

Acknowledgements

Not applicable.

Funding

The present study was supported by grants from the Zhejiang Province Basic Public Welfare Research Project

(grant no. GF18H160036), the General Program-Education Department of Zhejiang Province (grant no. Y201738393), the General Program-Department of Education of Zhejiang Province (grant no. Y202045370) and the Project of Hangzhou Science and Technology Commission (grant no. 20170533B66).

Availability of data and materials

The datasets used and/or analyzed during the current study are available from the corresponding author on reasonable request.

Authors' contributions

MZ and XC conceived and designed the study and wrote the manuscript. DC, PT, FW and YW performed the experiments and analyzed the datasets. JL and JZ performed flow cytometric analysis and edited the manuscript. DC and XC confirmed the authenticity of all the raw data. All authors read and approved the manuscript.

Ethics approval and consent to participate

Not applicable.

Patient consent for publication

Not applicable.

Competing interests

The authors declare that they have no competing interests.

References

1. Ferlay J, Shin HR, Bray F, Forman D, Mathers C and Parkin DM: Estimates of worldwide burden of cancer in 2008: GLOBOCAN 2008. Int J Cancer 127: 2893-2917, 2010.
2. Torre LA, Bray F, Siegel RL, Ferlay J, Lortet-Tieulent J and Jemal A: Global cancer statistics, 2012. CA Cancer J Clin 65: 87-108, 2015.
3. Ribeiro Pereira ACP, Koifman RJ and Bergmann A: Incidence and risk factors of lymphedema after breast cancer treatment: 10 years of follow-up. Breast 36: 67-73, 2017.
4. Lemler DJ, Lynch ML, Tesfay L, Deng Z, Paul BT, Wang X, Hegde P, Manz DH, Torti SV and Torti FM: DCYTB is a predictor of outcome in breast cancer that functions via iron-independent mechanisms. Breast Cancer Res 19: 25, 2017.
5. Cuzick J, DeCensi A, Arun B, Brown PH, Castiglione M, Dunn B, Forbes JF, Glaus A, Howell A, von Minckwitz G, *et al*: Preventive therapy for breast cancer: A consensus statement. Lancet Oncol 12: 496-503, 2011.
6. Weigelt B, Peterse JL and van't Veer LJ: Breast cancer metastasis: Markers and models. Nat Rev Cancer 5: 591-602, 2005.
7. Rinn JL and Chang HY: Genome regulation by long noncoding RNAs. Annu Rev Biochem 81: 145-166, 2012.
8. Hu YP, Jin YP, Wu XS, Yang Y, Li YS, Li HF, Xiang SS, Song XL, Jiang L, Zhang YJ, *et al*: LncRNA-HGBC stabilized by HuR promotes gallbladder cancer progression by regulating miR-502-3p/SET/AKT axis. Mol Cancer 18: 167, 2019.
9. Lin C and Yang L: Long noncoding RNA in cancer: Wiring signaling circuitry. Trends Cell Biol 28: 287-301, 2018.
10. Wang Z, Wang P, Cao L, Li F, Duan S, Yuan G, Xiao L, Guo L, Yin H, Xie D, *et al*: Long intergenic non-coding RNA 01121 promotes breast cancer cell proliferation, migration, and invasion via the miR-150-5p/HMGA2 axis. Cancer Manag Res 11: 10859-10870, 2019.
11. Guo S, Jian L, Tao K, Chen C, Yu H and Liu S: Novel breast-specific long non-coding RNA LINC00993 acts as a tumor suppressor in triple-negative breast cancer. Front Oncol 9: 1325, 2019.
12. Hu Q, Li C, Wang S, Li Y, Wen B, Zhang Y, Liang K, Yao J, Ye Y, Hsiao H, *et al*: LncRNAs-directed PTEN enzymatic switch governs epithelial-mesenchymal transition. Cell Res 29: 286-304, 2019.
13. Jin C, Yan B, Lu Q, Lin Y and Ma L: Reciprocal regulation of Hsa-miR-1 and long noncoding RNA MALAT1 promotes triple-negative breast cancer development. Tumour Biol 37: 7383-7394, 2016.
14. Xu X, Gu J, Ding X, Ge G, Zang X, Ji R, Shao M, Mao Z, Zhang Y, Zhang J, *et al*: LINC00978 promotes the progression of hepatocellular carcinoma by regulating EZH2-mediated silencing of p21 and E-cadherin expression. Cell Death Dis 10: 752, 2019.
15. Qian H, Chen L, Huang J, Wang X, Ma S, Cui F, Luo L, Ling L, Luo K and Zheng G: The lncRNA MIR4435-2HG promotes lung cancer progression by activating β-catenin signalling. J Mol Med (Berl) 96: 753-764, 2018.
16. Li X, Ren Y and Zuo T: Long noncoding RNA LINC00978 promotes cell proliferation and invasion in nonsmall cell lung cancer by inhibiting miR-6754-5p. Mol Med Rep 18: 4725-4732, 2018.
17. Wang H, Wu M, Lu Y, He K, Cai X, Yu X, Lu J and Teng L: LncRNA MIR4435-2HG targets desmoplakin and promotes growth and metastasis of gastric cancer by activating Wnt/β-catenin signaling. Aging (Albany NY) 11: 6657-6673, 2019.
18. Luo P, Wu SG, Ji KB, Yuan X, Li HM, Chen JP, Tian YF, Qiu Y and Zhong XM: LncRNA MIR4435-2HG mediates cisplatin resistance in HCT116 cells by regulating Nrf2 and HO-1. PLoS One 15: e0223035, 2020.
19. Zhu LJ, Wang AH, Gao M, Duan XY and Li ZH: LncRNA MIR4435-2HG triggers ovarian cancer progression by regulating miR-128-3p/CKD14 axis. Cancer Cell Int 20: 145, 2020.
20. Deng LL, Chi YY, Liu L, Huang NS, Wang L and Wu J: LINC00978 predicts poor prognosis in breast cancer patients. Sci Rep 6: 37936, 2016.
21. Livak KJ and Schmittgen TD: Analysis of relative gene expression data using real-time quantitative PCR and the 2(-Delta Delta C(T)) method. Methods 25: 402-408, 2001.
22. Tang Z, Li C, Kang B, Gao G, Li C and Zhang Z: GEPIA: A web server for cancer and normal gene expression profiling and interactive analyses. Nucleic Acids Res 45: W98-W102, 2017.
23. Pohl SG, Brook N, Agostino M, Arfuso F, Kumar AP and Dharmarajan A: Wnt signaling in triple-negative breast cancer. Oncogenesis 6: e310, 2017.
24. Liu S, Qiao Z, Ma Q, Liu X and Ma X: LncRNA CYTOR and MIR4435-2HG in ovarian cancer and its relationship with clinicopathological features. Panminerva Med 2019 (Epub ahead of print).
25. Zhang H, Meng H, Huang X, Tong W, Liang X, Li J, Zhang C and Chen M: lncRNA MIR4435-2HG promotes cancer cell migration and invasion in prostate carcinoma by upregulating TGF-β1. Oncol Lett 18: 4016-4021, 2019.
26. Hengartner MO: The biochemistry of apoptosis. Nature 407: 770-776, 2000.
27. McIlwain DR, Berger T and Mak TW: Caspase functions in cell death and disease. Cold Spring Harb Perspect Biol 5: a008656, 2013.
28. Degterev A, Boyce M and Yuan J: A decade of caspases. Oncogene 22: 8543-8567, 2003.
29. Suliman A, Lam A, Datta R and Srivastava RK: Intracellular mechanisms of TRAIL: Apoptosis through mitochondrial-dependent and -independent pathways. Oncogene 20: 2122-2133, 2001.
30. Lamouille S, Xu J and Derynck R: Molecular mechanisms of epithelial-mesenchymal transition. Nat Rev Mol Cell Biol 15: 178-196, 2014.
31. Thiery JP, Acloque H, Huang RY and Nieto MA: Epithelial-mesenchymal transitions in development and disease. Cell 139: 871-890, 2009.
32. Kalluri R and Weinberg RA: The basics of epithelial-mesenchymal transition. J Clin Invest 119: 1420-1428, 2009.
33. Wang YP, Guo PT, Zhu Z, Zhang H, Xu Y, Chen YZ, Liu F and Ma SP: Pleomorphic adenoma gene like-2 induces epithelial-mesenchymal transition via Wnt/β-catenin signaling pathway in human colorectal adenocarcinoma. Oncol Rep 37: 1961-1970, 2017.
34. Zhang P, Zhao X, Zhang W, He A, Lei B, Zhang W and Chen Y: Leukemia-associated gene MLAA-34 reduces arsenic trioxide-induced apoptosis in HeLa cells via activation of the Wnt/β-catenin signaling pathway. PLoS One 12: e0186868, 2017.

35. Shao HM, Ma JH, Guo TH and Hu RR: Triptolide induces apoptosis of breast cancer cells via a mechanism associated with the Wnt/β-catenin signaling pathway. Exp Ther Med 8: 505-508, 2014.
36. Knobloch J, Schmitz I, Götz K, Schulze-Osthoff K and Rüther U: Thalidomide induces limb anomalies by PTEN stabilization, akt suppression, and stimulation of caspase-dependent cell death. Mol Cell Biol 28: 529-538, 2008.
37. Yang M, He X, Huang X, Wang J, He Y and Wei L: LncRNA MIR4435-2HG-mediated upregulation of TGF-beta1 promotes migration and proliferation of nonsmall cell lung cancer cells. Environ Toxicol 35: 582-590, 2020.
38. Kong Q, Liang C, Jin Y, Pan Y, Tong D, Kong Q and Zhou J: The lncRNA MIR4435-2HG is upregulated in hepatocellular carcinoma and promotes cancer cell proliferation by upregulating miRNA-487a. Cell Mol Biol Lett 24: 26, 2019.